INVITED PAPER Special Section on Optical Signal-Processing Devices for Photonic Networks

Wavelength Conversion Using Quasi-Phase Matched $LiNbO_3$ Waveguides

Masaki ASOBE[†a)], **Yoshiki NISHIDA**[†], **Osamu TADANAGA**[†], **Hiroshi MIYAZAWA**[††], *Members*, *and* **Hiroyuki SUZUKI**[†], *Nonmember*

SUMMARY This paper describes recent progress in research on wavelength converters that employ quasi-phase-matched $LiNbO_3$ (QPM-LN) waveguides. The basic structure and operating principle of these devices are presented. The conversion efficiency in difference frequency generation (DFG), second harmonic generation (SHG) and an SHG/DFG cascade scheme are explained. Device fabrication technologies such as periodic poling, and those used for annealed proton-exchanged (APE) waveguides, and direct bonded waveguides are introduced. An APE waveguide is used to demonstrate the wavelength conversion of broadband (> 1 Tbit/s) WDM signals. The low penalty conversion of high-speed (40 Gbit/s) based WDM signals is also reported. Excellent resistance to photorefractive damage in a direct bonded waveguide is presented. This high level of resistance enabled highly efficient wavelength conversion. A new design concept is introduced for a multiple QPM device based on the continuous phase modulation of a periodically poled structure. This multiple QPM device enables the variable wavelength conversion of WDM signals. High-speed wavelength switching between ITU-T grid wavelengths using a finely tuned multiple QPM device is also reported. QPM-LN based wavelength converters have several advantages, including the ability to convert high-speed signals of 1 THz or greater, no signal-to-noise (S/N) ratio degradation, no modulation format dependence, and they are capable of the simultaneous conversion of broadband WDM channels. They will therefore be key devices in future photonic networks.

key words: *wavelength conversion, waveguide, lithium niobate, quasi-phase matching*

1. Introduction

In recent years, progress has been made on the development of technology for constructing large-capacity optical communications systems by the wavelength division multiplexing of high-speed optical signals. The flexible and efficient use of a future network requires photonic network technology that allows optical signals to be processed in a simple manner without the need to convert them to electrical signals. Much is expected from wavelength conversion devices in terms of making such technology possible. Various types of wavelength conversion device have been proposed and studied, but the device described here, which employs quasi-phase-matched $LiNbO_3$ (QPM-LN) waveguides, has superior features to these other devices, including the ability to convert high-speed signals of 1 THz or greater, no signal to noise (S/N) ratio degradation, no signal format dependence, and the capacity to convert a group of broadband wavelengths simultaneously [1].

Here, we describe the operating principle and report recent advances in wavelength conversion realized using the QPM-LN waveguide.

2. Principle of Wavelength Conversion

Wavelength conversion using QPM-LN waveguides is based on difference frequency generation (DFG). By injecting a signal light that has a frequency ω_1 (wavelength $\lambda_1 = 2\pi c/\omega_1$) and a pump light that has a frequency ω_3 (wavelength $\lambda_3 = 2\pi c/\omega_3$) into a second-order nonlinear material, this effect can be used to generate a converted light that has a wavelength ($\lambda_2 = 2\pi c/\omega_2$), which is equivalent to the difference between the frequencies of the two beams, $\omega_2 = \omega_3 - \omega_1$. To achieve highly efficient conversion, it is essential to satisfy the phase matching condition. Quasi-phase-matching (QPM) is a technique that relaxes the phase matching constraint and allows the wavelength conversion of arbitrary wavelength combinations in the wavelength region where the material is transparent. With the QPM wavelength conversion technique, the nonlinear coefficient is modulated with period Λ, so that the value of the phase mismatch, $\Delta\beta$, satisfies the following equation.

$$\Delta\beta = 2\pi\left(\frac{n_3}{\lambda_3} - \frac{n_2}{\lambda_2} - \frac{n_1}{\lambda_1}\right) = 2\pi\left(\frac{1}{\Lambda}\right) \tag{1}$$

(Here, n_1 is the refractive index at the signal light wavelength λ_1, n_2 is the refractive index at the converted light wavelength, λ_2, and n_3 is the refractive index at the pump light wavelength, λ_3.) This is the quasi-phase-matching condition. Using this technique, we can achieve highly efficient conversion between various wavelengths by varying the modulation period. The basic structure of the device is shown in Fig. 1(a). An optical waveguide is formed on a substrate on which a QPM structure has been formed by periodically reversing the spontaneous polarization of the $LiNbO_3$. Figures 1(b) and (c) show a typical arrangement of the signal light, the pump light and the converted light on the wavelength axis. For conversion from the 1.55 μm band to the 1.58 μm band, for example, the signal light and a 0.78 μm pump light are injected into the waveguide. The wavelength conversion efficiency as a function of the phase mismatching of Eq. (1) is given by Eq. (2).

Manuscript received July 29, 2004.
Manuscript revised September 25, 2004.

[†]The authors are with NTT Photonics Laboratories, NTT Corporation, Atsugi-shi, 243-0198 Japan.
[††]The author is with NTT Electronics Corporation, Atsugi-shi, 243-0198 Japan.
a) E-mail: m-asobe@aecl.ntt.co.jp

DOI: 10.1093/ietele/e88–c.3.335

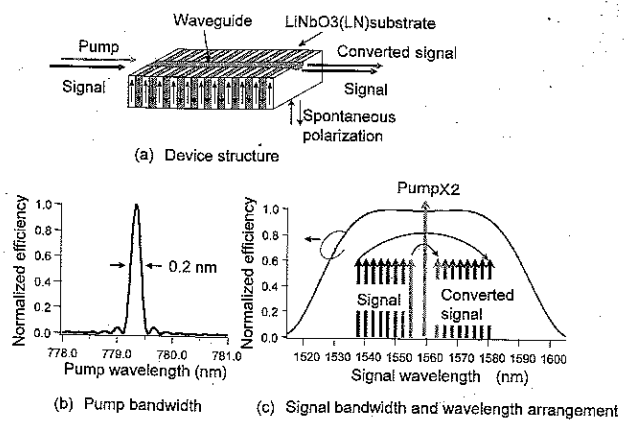

Fig. 1 Structure and operating principle of QPM-LN wavelength converter.

$$\eta_L = \eta_{\max} \frac{\sin\left[\left(\Delta\beta - \frac{2\pi}{\Lambda}\right)\frac{L}{2}\right]^2}{\left[\left(\Delta\beta - \frac{2\pi}{\Lambda}\right)\frac{L}{2}\right]^2} \tag{2}$$

($\eta_{\max}$ is the efficiency under the QPM condition and L is waveguide length.)

Figure 1 also shows the dependence of the wavelength conversion efficiency on the pump and signal wavelengths when a 30 mm long LN waveguide is used. As seen in Eq. (2), the bandwidth of the device is determined by the condition whereby $(\Delta\beta - 2\pi/\Lambda)L$ remains between $-\pi$ to $+\pi$. When the pump wavelength changes, the $\Delta\beta$ changes sharply due to the dispersion in the refractive index of LN. Thus, the bandwidth for the pump wavelength, as shown in Fig. 1(b), is as narrow as 0.2 nm. By contrast, when the pump wavelength is fixed and the signal wavelength becomes longer, for example, the converted signal wavelength becomes shorter. Thus, the changes in the refractive index at the signal and converted signal wavelengths cancel each other out and result in a small change in $\Delta\beta$. This is why conversion is possible over a very wide signal wavelength range (60 nm), as shown in Fig. 1(c). This sufficiently wide bandwidth makes the batch conversion of the WDM signal possible. In addition, conversion can be accomplished easily, even for high-speed signals of, for example, 40 Gbit/s or more.

Furthermore, because the phase information of the input signal light is preserved in the conversion process, it is independent of the modulation format, even for signals that take full advantage of phase modulation. Another merit of the QPM-LN device is that low noise is added to the optical signal in the wavelength conversion process, because the device itself produces virtually no spontaneous emission.

For 1.55 μm band wavelength conversion as described above, a 0.78 μm light source is required for the pump light. However, there are few laser diodes that emit a single wavelength in this wavelength band. It is possible, however, to use a 1.55 μm light source as an external pump light with a cascade scheme [2]. In that scheme, a 1.55 μm light injected into the waveguide as an external pump light is converted into a 0.78 μm internal pump light by second harmonic generation (SHG). Wavelength conversion is achieved by the DFG of that internal pump light and the signal light. As regards the SHG process, the wavelength of the 1.55 μm pump light is consistent with the degenerative wavelength, at which the signal and converted signal wavelengths converge in the DFG process. Thus, the QPM conditions for the SHG and DFG processes are satisfied simultaneously by the same poling period, and the generation of the internal pump light by SHG and the wavelength conversion by DFG can be accomplished in the same waveguide.

Next, we consider the wavelength conversion efficiency. If the attenuation of the pump light in the DFG process is negligible (small signal approximation), the power of the converted light, P_2, is given by Eq. (3) in terms of the signal light power, P_1, and the pump light power, P_3.

$$P_2 = \frac{\eta L^2 P_1 P_3}{100} \tag{3}$$

Here, η represents the conversion efficiency per unit length of the device, and is expressed in units of %/W/cm^2. The overall efficiency of the device, ηL^2, improves in proportion to the square of the waveguide length, and is expressed in units of %/W.

If we disregard the mode overlap between the three interacting waves, the conversion efficiency is given by Eq. (4).

$$\eta L^2 = 100 \frac{8\pi^2 d_{eff}^2}{n_1 n_2 n_3 c \varepsilon_0 \lambda_1^2 A_{eff}} L^2 \tag{4}$$

Here, $d_{eff} = 2d_{33}/\pi$ is the effective nonlinear coefficient, c is the velocity of light, ε_0 is the vacuum permittivity, and A_{eff} is the effective mode area. If we assume the nonlinear optical coefficient d_{33}=28 pm/V, L=50 mm, A_{eff}=19.6 μm^2 (mode diameter=5.0 μm), and λ_1=1.55 μm, we can expect a conversion efficiency as high as 5000%/W. In actual devices, the conversion efficiency is affected by several factors including the mode overlap between three interacting waves, nonlinearity degradation during waveguide processing, and the non-uniformity of the waveguide.

With the SHG process, if we assume that the attenuation due to the wavelength conversion of the fundamental wavelength can be disregarded (small signal approximation), the power of the SH light, P_3, is given in terms of the power of the fundamental wave, P_4, by Eq. (5).

$$P_3 = \frac{\eta L^2 P_4^2}{100} \tag{5}$$

The efficiency in the SHG process is the same as in the DFG process. Therefore, SHG conversion efficiency is used to evaluate the conversion efficiency of the device.

In the cascade scheme the power of the converted light, P_2, is given by Eq. (6).

$$P_2 = \frac{1}{4}\frac{\eta^2 L^4 P_1 P_4^2}{100^2} \tag{6}$$

Here we assumed a small signal approximation. The internal SH pump light is proportional to the square of the external pump light power, and so the increase in the power of the converted light with the cascade scheme is proportional to the square of the pump light power.

Most QPM-LN waveguide devices utilize the nonlinear optical coefficient of d_{33}, which is the largest component in $LiNbO_3$. Thus the pump and signal polarizations should coincide with the Z axis of the crystal. This means the wavelength converter is polarization dependent. To overcome this problem, polarization diversity using two identical waveguides [1], single waveguide in a loop configuration [1], and single waveguide with polarization rotation have been proposed [3].

3. Device Fabrication and Wavelength Conversion Characteristics

3.1 Fabrication Technology

$LiNbO_3$ with a periodically reversed polarization is called periodically poled lithium niobate (PPLN). Various methods have been used in attempts to fabricate such structures, but in recent years a method has been established that involves the direct application of an electric field to the substrate [4].

We have been employing two waveguide fabrication methods. One is the annealed proton exchange (APE) method [5]. With this method, first a mask pattern of SiO_2 or other such material is formed photolithographically on the LN substrate, and then the substrate is immersed in a proton donor such as benzoic acid at a high temperature to form a high-index layer on the substrate by the exchange of Li^+ and H^+ ions. Excessively exchanged proton causes a crystal phase transition, which reduces the nonlinearity of the crystal. To recover the nonlinearity, the exchanged protons are diffused by annealing. With this method we can obtain a large change in the refractive index and thus achieve strong optical confinement. This method features a relatively simple process and provides the ability to fabricate waveguides over a large surface area with good uniformity. We have already succeeded in fabricating a 5 cm long waveguide device that has an SHG efficiency of 1300%/W. Recently, a more efficient device has been developed by using the reverse proton exchange method [6]. The APE method is also known to have better robustness against photorefractive damage than the Ti diffusion method used for LN optical modulators [7]. To date, most $LiNbO_3$ waveguides for wavelength conversion applications have been fabricated by the APE method [1], [5], [6]. Although this method is well established, additional defects could be induced in the crystal during the process. In general, defects in nonlinear optical crystal reduce the robustness of the device against photorefractive damage.

To solve this problem we tried to make a waveguide using the crystal without proton exchange [8]. Figure 2 shows our fabrication process based on the direct bonding technique. Z-cut non-doped or Zn-doped LN is used for the

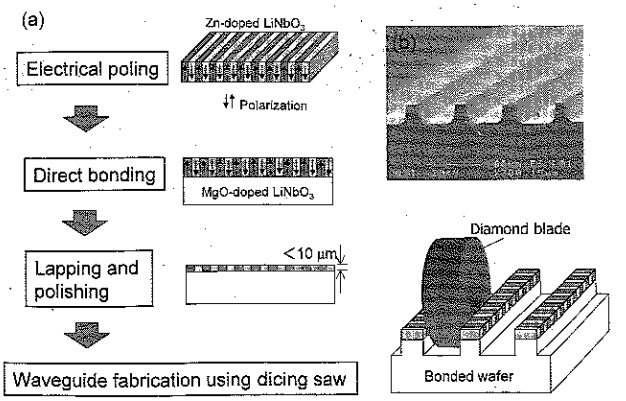

Fig. 2 Waveguide fabrication using direct bonding technology.

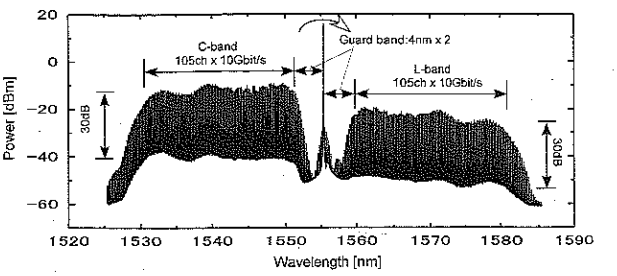

Fig. 3 Spectrum of broadband wavelength conversion.

core wafer and Z-cut Mg-doped LN is used for the cladding wafer. First, a periodically poled structure is formed on the core wafer by using the electrical poling method. Then, the two wafers are brought into contact in a clean atmosphere and annealed at 500°C to achieve complete bonding at the atomic level. The thickness of the core layer was reduced to a few microns by lapping and polishing. The ridge waveguides were then fabricated by using a dicing saw. The inset in Fig. 2 shows a cross-sectional view of the fabricated ridge waveguides. By choosing an ultra fine diamond blade for the dicing, we succeeded in obtaining a flat and smooth waveguide surface without the need for chemical etching or polishing. Recently, we successfully used this method to fabricate a 50 mm-long waveguide with an SHG efficiency of 560%/W [9].

3.2 Wavelength Conversion Demonstration Using Annealed Proton Exchange (APE) Waveguide

In this section, we introduce recent progress on a wavelength converter that employs the APE method. To facilitate stable wavelength conversion, we have fabricated a QPM-LN waveguide module that has fiber pigtails for the input and output as well as a temperature control function for QPM wavelength adjustment [10]. We used the module in an attempt to demonstrate the merits of a wavelength converter based on the QPM-LN waveguide. Figure 3 shows the spectrum of our broadband wavelength conversion experiment. Here, 1.03 Tbit/s (103 × 10 Gbit/s), 25 GHz-spaced DWDM signals (1531–1551 nm) were generated by modu-

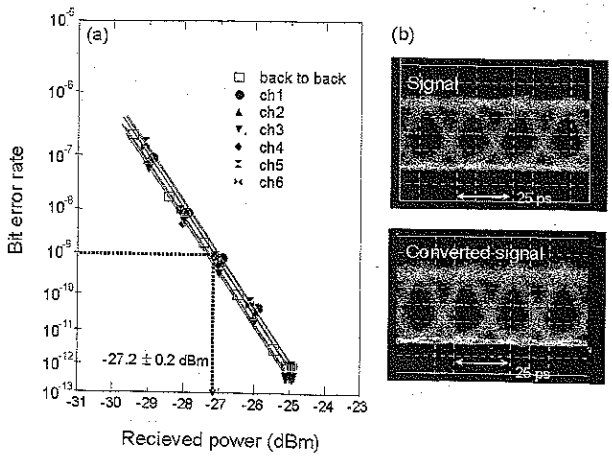

Fig. 4 (a) Bit error performance and (b) eye diagram of 40 Gbit/s signals.

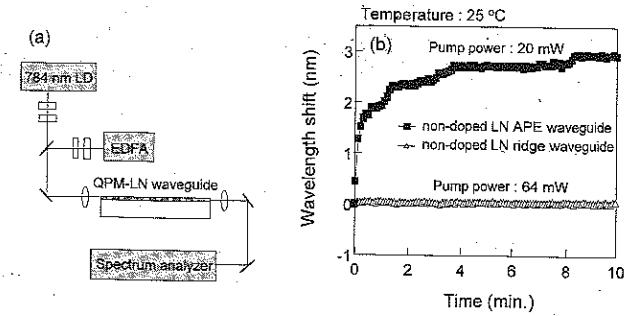

Fig. 5 (a) Experimental setup for photo-refractive damage measurement and (b) QPM wavelength shift as a function of irradiation time.

lating a supercontinuum light source [11]. Broadband signals in the C-band were converted to the L-band in a pigtailed QPM-LN module by using a cascade scheme. The wide signal bandwidth made large-capacity signal wavelength conversion possible in a single device. If the signal wavelength is assigned within the QPM bandwidth for the pump, parametric crosstalk may degrade the signal quality. The narrow pump bandwidth allowed us to achieve conversion with a narrow guard band of 8 nm.

To confirm the ability to convert high-speed signals we also attempted the wavelength conversion of WDM signals on six 40-Gbit/s channels [10]. Figure 4 shows the input optical signal, the eye pattern of the converted light, and the bit error rates before and after wavelength conversion. As seen in this diagram, there was no waveform degradation after wavelength conversion in this device. Furthermore, the power penalty after wavelength conversion was 0.3 dB, that is, barely within the limits of measurement, which confirms that the noise introduced by the wavelength conversion process is negligible.

3.3 Highly Damage Resistant Device Using Direct Bonded Waveguide

In this section, we introduce recent progress on a device that uses a direct bonded waveguide. One of the most significant features of the direct bonded waveguide is its strong resistance to photorefractive damage. When a high-power light is injected into a second-order nonlinear crystal such as LN, a change in the index of refraction occurs because of a photorefractive effect in which the carrier is excited, mainly as a result of the presence of defects in the crystal. If there is a change in the index of refraction in a device that employs QPM, the QPM conditions obtained with Eq. (1) change and this leads to a change in the QPM wavelength. In DFG wavelength conversion, the pump wavelength band is relatively narrow, as shown in Fig. 1, so the change in the QPM wavelength may reduce the conversion efficiency. Even in APE waveguides slight photorefractive damage causes a QPM wavelength shift. It is known that doping LN with Mg or Zn increases the robustness against photorefractive damage by compensating for the carrier created by the defects [7]. However even if an MgO- or ZnO-doped LN substrate is used, the QPM wavelength shift of the APE waveguide cannot be eliminated at room temperature [11].

To evaluate the improvement in robustness against photorefractive damage, we measured the change in the QPM wavelength when we injected a light with a short wavelength near that of the pump. The experimental setup is shown in Fig. 5(a) [12]. When the broadband ASE from an erbium-doped fiber amplifier (EDFA) is injected into the QPM-LN device, only the wavelength component that matches the QPM wavelength is converted by SHG. Accordingly, by observing the spectrum in the 0.78 μm band with an optical spectrum analyzer, a QPM curve, such as that shown in Fig. 1(b), can be measured instantaneously. The temporal change in the QPM wavelength can be measured by monitoring the SH spectrum at constant intervals while injecting a 784 nm light beam, which is slightly detuned from the QPM wavelength. Figure 5(b) shows the temporal change in QPM wavelength at room temperature. We compared an APE waveguide made of non-doped LN and with a direct bonded waveguide made of non-doped LN as a core layer [8]. The APE waveguide exhibited an appreciable wavelength shift of 3 nm with an irradiation power of 20 mW. In contrast, the direct bonded ridge waveguide showed no wavelength shift even with an irradiation power of 64 mW. This very high resistance to photorefractive damage will be beneficial in terms of realizing practical QPM-LN wavelength converters.

In the DFG process, if sufficient pump power is injected, the intensity of the converted signal can reach the signal input level. If a larger pump power is injected, parametric amplification of both the signal and the converted signal is possible. We conducted a wavelength conversion experiment using a direct bonded waveguide made of Zn-doped LN as a core layer [9]. A 1535 nm signal light and a 1546 nm pump light amplified by the EDFA were combined by a fiber coupler and injected into the waveguide. The output spectrum with a pump power of 150 mW is shown in Fig. 6(a). The difference between the output levels of the signal and converted signal was as little as −1.3 dB. Figure 6(b) shows

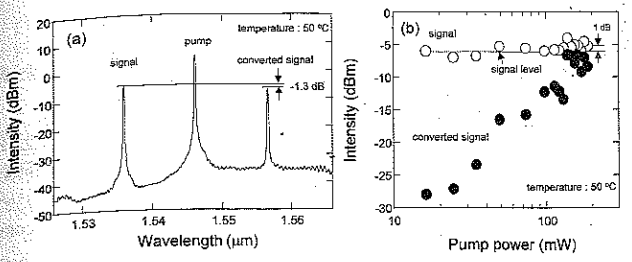

Fig. 6 (a) Spectrum of wavelength conversion using direct bonded waveguide and (b) output intensity as a function of pump power.

the output intensities of the signal and converted signal as a function of the pump power. The converted signal increases in proportion to the square of the pump power. Thanks to the high damage resistance of the Zn-doped direct bonded waveguide, there was no saturation in the conversion efficiency caused by the QPM wavelength shift [13]. Although the SNR of the converted signal in Fig. 6(a) is limited by the ASE generated from he EDFA, low loss wavelength conversion without SNR degradation will be possible by using an appropriate band pass filter.

Another advantage of the direct bonded waveguide is that it can confine both the TE and TM modes. The APE waveguides can confine only the TM mode when the substrate is Z-cut $LiNbO_3$. If the waveguide can confine both polarizations, polarization-independent operation can be achieved by polarization diversity using a polarization rotation [3]. In addition, it is known that excessive proton exchange induces a "dead layer" whose nonlinearity is largely degraded [5]. The direct bonded waveguide does not suffer from nonlinearity degradation. We expect to achieve more efficient wavelength conversion by optimizing the waveguide structure.

4. Variable Wavelength Conversion Using Multiple QPM Device

A conventional periodically poled structure provides a phase matching curve with a single QPM peak. If we have multiple QPM peaks, we can change the destination wavelength by changing the pump wavelength. Several engineered domain structures have been proposed with a view to realizing a multiple QPM device. These include a periodic phase reversal structure [14] and an aperiodic optical superlattice structure [15]. Recently we devised a novel technique that can achieve multiple QPM with better efficiency than that provided by the previous technique [16]. Figure 7(a) shows a schematic of the domain structure. In this structure, the sign of $\chi^{(2)}$ is alternated with a period Λ_0, whereas the phase of $\chi^{(2)}$ alternation is continuously modulated with a period Λ_{ph}, as shown in Fig. 7(b). Fourier transform analysis shows that this structure provides multiple QPM when the phase mismatch $\Delta\beta$ satisfies the following condition:

$$\Delta\beta = 2\pi\left(\frac{1}{\Lambda_0} + \frac{n}{\Lambda_{ph}}\right) \tag{7}$$

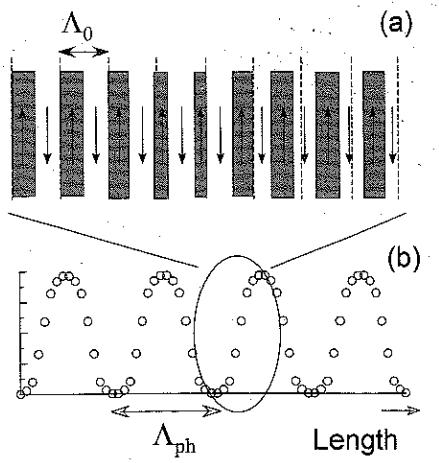

Fig. 7 (a) Schematic of continuously phase modulated $\chi^{(2)}$ grating and (b) its periodic phase modulation function.

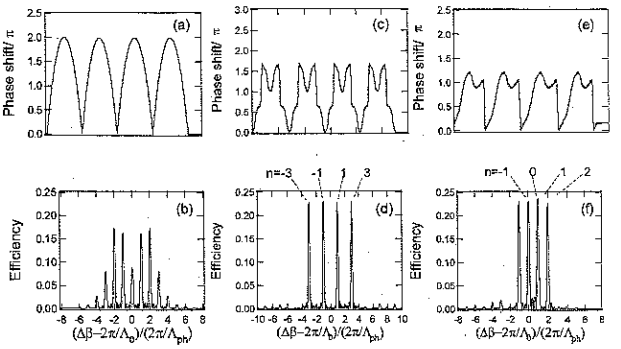

Fig. 8 Phase-modulation functions and QPM curves for (a), (b) parabolic function; (c), (d) symmetrically optimized 4-channel device; (e), (f) asymmetrically optimized 4-channel device.

where n is an integer number.

For example, if we choose a parabolic phase modulation function as shown in Fig. 8(a), the phase matching curve exhibits multiple peaks with unequal efficiency as shown in Fig. 8(b). To achieve multiple QPM with high efficiency, we began with the parabolic function and then optimized the phase modulation function so that only the efficiency with the desired n numbers was maximized. Figures 8(c) and (d) show examples of the phase modulation and the phase matching curves optimized for 4-ch pumping. The efficiency was normalized using that of a uniform phase structure with the same interaction length. In this case, efficiencies with four odd n numbers ($n = -3, -1, 1, 3$) were maximized to obtain even peaks. The normalized efficiency of each peak is 23.5%, which means the sum of the efficiencies for the desired peaks is 94%. As shown in Fig. 8(d), unwanted side lobes in the phase matching curve are effectively suppressed. This suppression results in better efficiency than that achieved using previously reported techniques. Figures 8(e) and (f) provide another example of the phase modulation and phase matching curves. Here, we optimized the phase modulation so that the efficiencies with asymmetrically arranged peaks ($n = -1, 0, 1, 2$) were max-

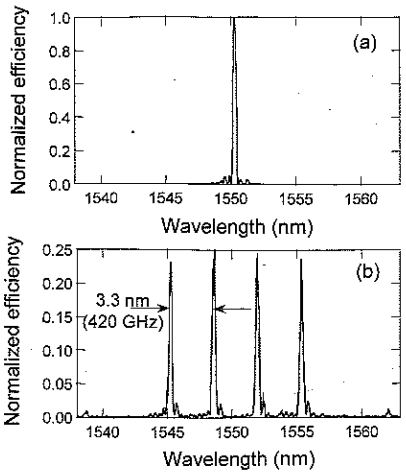

Fig. 9 Experimentally measured SHG tuning curves for a device with (a) uniform and (b) phase-modulated domain structure.

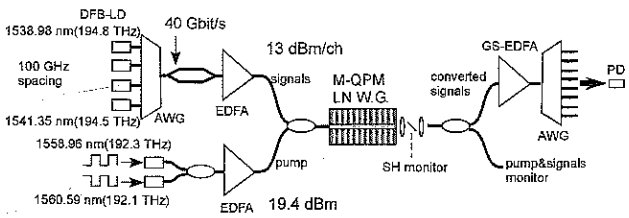

Fig. 10 Experimental setup for wavelength switching.

imized [17]. By employing the asymmetric phase modulation function, we can halve the peak interval using the same phase modulation period. In the same manner, this technique can be extended to any number of pump wavelengths by obtaining an appropriate optimum phase modulation function. Based on this design concept, we fabricated a prototype waveguide-device using the conventional APE method.

Figures 9(a) and (b) show normalized SHG tuning curves for a conventional periodically poled sample and a phase modulated sample. Both samples were 34.5 mm long. The peak SHG efficiency of the conventional periodically poled sample was 680%/W. The experimental and calculated tuning curves of the phase modulated sample are in good agreement (Fig. 8(d)), and an SHG efficiency of 160%/W was obtained from each peak.

For conversion between two waves on the ITU-T grid, the pump frequency should be on the grid or in the middle of the grid. Consequently, each multiple QPM peak should fit the ITU-T grid or the middle. Recently, we fine-tuned the multiple-QPM device [18] and then used it to demonstrate conversion between ITU-T grid wavelengths and the high-speed switching of the converted wavelength. Figure 10 shows the experimental setup. C-band 4-channel DFB-LDs with a 100 GHz spacing were multiplexed and modulated at 40 Gbit/s. Two-channel DFB-LDs with a 200 GHz spacing were directly modulated to generate a complementary pump pulse. The pump and signals were amplified by EDFAs, combined by a WDM coupler, and then launched into the multiple-QPM $LiNbO_3$ waveguide.

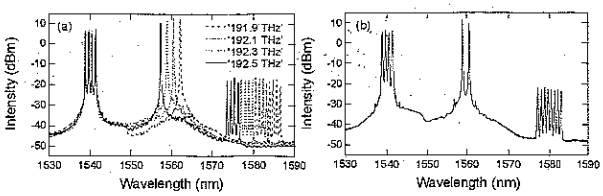

Fig. 11 Output spectra with (a) 4 different pump wavelengths, (b) complementarily modulated 2 ch pump.

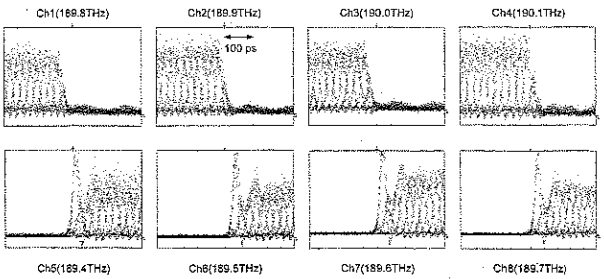

Fig. 12 Temporal waveform of high speed wavelength switching.

Figure 11(a) shows output spectra with four different pump wavelengths. By changing the pump frequency by 200 GHz, we were able to demonstrate the variable and simultaneous wavelength conversion of 4-ch 100 GHz spacing signals. Next, we tried high-speed wavelength switching using complementarily modulated pump light. Figure 11(b) shows the averaged output spectrum. In this case, a 4-ch 100 GHz spacing signal is complementarily converted into two groups of 4-ch 100 GHz spacing signals. Figure 12 shows the temporal waveforms of converted signals. The 4-ch signal was properly converted to 2×4-ch signals on the ITU-T grid frequency. High-speed switching between 4-ch 100-GHz-spacing signal groups is also successfully demonstrated. Taking the transition effect into account, fast wavelength switching would be possible with a guard time as short as 100 ps. These fast wavelength switching characteristics would be useful in achieving burst/packet routing based on high-speed signals.

The multiple QPM device technology may play an essential role in the wavelength routing of grouped WDM signals in future photonic networks.

5. Conclusion

We have provided an overview of QPM wavelength conversion devices and the current state of research. Although we have introduced QPM-LN devices from the viewpoint of wavelength conversion, a wide variety of other applications such as dispersion compensation, [1] and time division multi/demultiplexing [19] have been reported. We believe that the high efficiency, broad bandwidth, high SNR, transparency and other excellent characteristics possessed by these devices ensure that their importance will continue to grow.

Acknowledgments

The authors thank J. Yamawaku, A. Takada, T. Morioka and their colleagues for their collaboration in system application research.

References

[1] M.H. Chou, K.R. Parameswaran, M.M. Fejer, and I. Brener, "Optical signal processing and switching with second-order nonlinearities in waveguides," IEICE Trans. Electron., vol.E83-C, no.6, pp.869–874, June 2000.

[2] K. Gallo, F. Assanto, and G.I. Stegeman, "Efficient wavelength shifting over the erbium amplifier bandwidth via cascaded second order processes in lithium niobate waveguides," Appl. Phys. Lett., vol.71, pp.1020–1022, 1997.

[3] M. Asobe, H. Miyazawa, O. Tadanaga, Y. Nishida, and H. Suzuki, "Highly damage resistant Zn:$LiNbO_3$ ridge waveguide and its application to a polarization independent wavelength converter," IEEE J. Quantum Electron., vol.39, no.10, pp.1327–1333, 2003.

[4] M. Yamada, N. Nada, M. Saitoh, and K. Watanabe, "First-order quasi-phase matched $LiNbO_3$ waveguide periodically poled by applying an external field for efficient blue second-harmonic generation," Appl. Phys. Lett., vol.62, pp.435–436, 1993.

[5] M.L. Borz, L.A. Eyres, and M.M. Fejer, "Depth profiling of the d_{33} nonlinear coefficient in annealed proton exchanged $LiNbO_3$ waveguides," Appl. Phys. Lett., vol.62, pp.2012–2014, 1993.

[6] K.R. Parameswaran, R.K. Route, J.R. Kurz, R.V. Rosussev, M.M. Fejer, and M. Fujimura, "Highly efficient second-harmonic generation in buried waveguides formed by annealed and reverse proton exchange in periodically poled lithium niobate," Opt. Lett., vol.27, pp.179–181, 2002.

[7] M. Minakata, "$LiNbO_3$ optical waveguide device," IEICE Trans. Electron. (Japanese Edition), vol.J77-C-I, no.5, pp.194–205, May 1994.

[8] Y. Nishida, H. Miyazawa, M. Asobe, O. Tadanaga, and H. Suzuki, "A direct-bonded QPM-LN ridge waveguide with high damage resistance at room temperature," Electron. Lett., vol.39, pp.609–610, 2003.

[9] Y. Nishida, H. Miyazawa, M. Asobe, O. Tadanaga, and H. Suzuki, "Efficient parametric wavelength conversion using direct-bonded QPM-ZnO-doped $LiNbO_3$ waveguide," Technical Digest of Conf. on Lasers and Electro-Optics, no.CFA1, San Francisco, May 2004.

[10] M. Asobe, H. Miyazawa, O. Tadanaga, Y. Nishida, and H. Suzuki, "40 Gbit/s × 6 channel wavelength conversion using a quasi-phase matched $LiNbO_3$ waveguide module," OECC 2002, no.PD2-8, Yokohama, July 2002.

[11] J. Yamawaku, H. Takara, T. Ohara, K. Sato, A. Takada, T. Morioka, O. Tadanaga, H. Miyazawa, and M Asobe, "Inter-band wavelength conversion of 25 GHz-spaced 1.03 Tbit/s (103 × 10 Gbit/s) DWDM signals with small guard band and low crosstalk in PPLN waveguide," Technical Digest of Conf. on Lasers and Electro-Optics, no.CThPDB, Baltimore, June 2003.

[12] M. Asobe, O. Tadanaga, T. Yanagawa, H. Itoh, and H. Suzuki, "Reducing photorefractive effect in periodically poled ZnO- and MgO-doped $LiNbO_3$ wavelength converters," Appl. Phys. Lett., vol.78, pp.3163–3165, 2001.

[13] M. Asobe, O. Tadanaga, H. Miyazawa, and H. Suzuki, "Parametric wavelength conversion and amplification using damage-resistant Zn:$LiNbO_3$ waveguide," Electron. Lett., vol.37, pp.62–964, 2001.

[14] M.H. Chou, K.R. Parameswaran, M.M. Fejer, and I. Brener, "Multiple-channel wavelength conversion by use of engineered quasi-phase-matching structures in $LiNbO_3$ waveguides," Opt. Lett., vol.24, pp.1157–1159, 1999.

[15] Y.W. Lee, F.C. Fan, Y.C. Huang, B.Y. Gu, B.Z. Dong, and M.H. Chou, "Nonlinear multiwavelength conversion based on an aperiodic optical superlattice in lithium niobate," Opt. Lett., vol.27, pp.2191–2193, 2002.

[16] M. Asobe, O. Tadanaga, H. Miyazawa, Y. Nishida, and H. Suzuki, "Multiple quasi-phase-matched $LiNbO_3$ wavelength converter using a continuously-phase-modulated domain structure," Opt. Lett., vol.28, pp.558–561, 2003.

[17] M. Asobe, O. Tadanaga, H. Miyazawa, Y. Nishida, and H. Suzuki, "Flexible and robust multiple quasi-phase matched $LiNbO_3$ wavelength converter," Technical Digest of Conf. on Lasers and Electro-Optics, no.CWB3, Baltimore, June 2003.

[18] M. Asobe, O. Tadanaga, H. Miyazawa, Y. Nishida, and H. Suzuki, "High-speed wavelength switching of 40-Gb/s-based WDM signals using a multiple-QPM $LiNbO_3$ waveguide tailored for the ITU-T grid," OFC 2002, no.FL5, Anaheim, Feb. 2002.

[19] S. Kawanishi, T. Morioka, M.H. Chou, M.M. Fejer, and K. Fujiura, "All-optical modulation and time-division-multiplexing of 100 Gbit/s signal using quasi-phase-matched mixing in $LiNbO_3$ waveguides," Electron. Lett., vol.36, pp.1568–1569, 2000.

Masaki Asobe received B.S. and M.S. degrees in instrumentation engineering from Keio University, Kanagawa, Japan, in 1987 and 1989, respectively. He received a Ph.D. for work in nonlinear optics from the same university in 1995. In 1989, he joined NTT Laboratories, Kanagawa, Japan, where he has been engaged in research on nonlinear optical devices such as ultrafast all-optical switches and broadband wavelength converters as well as high-speed optical communication systems.

Yoshiki Nishida received B.S. and M.S. degrees in applied physics from Hokkaido University, in 1988 and 1990. He received a Ph.D. for work in optical-fiber amplifier technology from the same university in 1999. He joined NTT Laboratories, Ibaraki, Japan, in 1990, where he has been engaged in research on fluoride glass fibers. Since 1993, he has been engaged in developmental research on optical fiber amplifiers. He is currently engaged in research on quasi-phase-matched $LiNbO_3$ wavelength converters.

Osamu Tadanaga received B.E. and M.E. degrees in material science and engineering from Kyoto University, Kyoto, Japan, in 1993 and 1995, respectively. Since joining NTT Opto-electronics Laboratories, Kanagawa, Japan, in 1995, he has been engaged in research on surface-normal modulators, VCSELs, and quasi-phase-matched $LiNbO_3$ wavelength converters.

Hiroshi Miyazawa received B.E. and M.E. degrees in electrical and electronics engineering from the University of Chiba, Chiba, Japan, in 1982 and 1984, respectively. After joining the Electrical Communications Laboratories, Nippon Telegraph and Telephone Corporation (NTT), Tokyo, in 1984, he worked on optical components such as laser diode modules, external modulators, switches and wavelength converters for optical transmission systems.

Hiroyuki Suzuki received B.S., M.S. degrees and a Ph.D. in chemistry from the University of Tokyo, Japan, in 1981, 1983 and 1986, respectively. Since 1986, he has been with the R&D Laboratories of Nippon Telegraph and Telephone Corporation (NTT). He is currently the leader of the All-optical Processing Research Group of NTT Photonics Laboratories, and is in charge of the development of various types of optical functional materials and devices ranging from organics, and semiconductors to $LiNbO_3$ for use in future photonic communication and information processing.